A proposal for removing πN-state contamination from the nucleon induced pseudoscalar form factor in lattice QCD

Shoichi Sasaki,[a,*] **Yasumichi Aoki,**[b] **Ken-Ichi Ishikawa,**[c] **Yoshinobu Kuramashi,**[d] **Kohei Sato,**[e] **Eigo Shintani,**[d] **Ryutaro Tsuji,**[f] **Hiromasa Watanabe**[g] **and Takeshi Yamazaki**[h,d]

(PACS Collaboration)

[a]*Department of Physics, Tohoku University, 980-8578, Sendai, Japan*

[b]*RIKEN Center for Computational Science, 650-0047, Kobe, Japan*

[c]*Core of Research for the Energetic Universe, Graduate School of Advanced Science and Engineering, Hiroshima University 739-8526, Higashi-Hiroshima, Japan*

[d]*Center for Computational Sciences, University of Tsukuba, 305-8577, Tsukuba, Japan*

[e]*Degree Programs in Pure and Applied Sciences, Graduate School of Science and Technology, University of Tsukuba, Ibaraki 305-8571, Japan*

[f]*High Energy Accelerator Research Organization (KEK), 305-0801, Tsukuba, Japan*

[g]*Yukawa Institute for Theoretical Physics, Kyoto University, Kyoto 606-8502, Japan*

[h]*Institute of pure and Applied Sciences, University of Tsukuba, 305-8571, Tsukuba, Japan*

E-mail: ssasaki@nucl.phys.tohoku.ac.jp

In the PACS10 project, the PACS collaboration has generated three sets of the PACS10 gauge configurations at the physical point with lattice volume larger than $(10 \text{ fm})^4$ and three different lattice spacings. The isovector nucleon form factors had been already calculated by using two sets of the PACS10 gauge configurations. In our strategy, the smearing parameters of the nucleon interpolation operator were highly optimized to eliminate as much as possible the contribution of excited states in the nucleon two-point function. This strategy was quite successful in calculations of the electric (G_E), magnetic (G_M) and axial-vector (F_A) form factors, while the induced pseudoscalar (F_P) and pseudoscalar (G_P) form factors remained strongly affected by residual contamination of πN-state contribution. In this work, we propose a simple method to remove the πN-state contamination from the F_P form factor, and then evaluate the induced pseudoscalar charge g_P^* and the pion-nucleon coupling $g_{\pi NN}$ from existing data in a new analysis. Applying this method to the G_P form factor is also considered with a help of the axial Ward-Takahashi identity.

The 41st International Symposium on Lattice Field Theory (LATTICE2024)
28 July - 3 August 2024
Liverpool, UK

---

*Speaker

1. Introduction

The axial structure of the nucleon is highly connected with the physics of chiral symmetry and its spontaneous breaking, which ensures the presence of pseudo Nambu-Goldstone particles such as the pion. This is empirically known as the partially conserved axial-vector current (PCAC) hypothesis, where the divergence of the axial-vector current is proportional to the pion field. Applying this idea to the axial-vector matrix element of the nucleon given by

$$\langle N(p')|A_\alpha(x)|N(p)\rangle = \bar{u}_N(p')\left[\gamma_\alpha\gamma_5 F_A(q^2) + iq_\alpha\gamma_5 F_P(q^2)\right]u_N(p)e^{iq\cdot x} \tag{1}$$

with $q = p' - p$, a specific relation, known as the Goldberger-Treiman (GT) relation [1], is derived between the axial-vector coupling defined by the axial-vector (F_A) form factor at $q^2 = 0$ and the residue of the pion-pole structure in the induced pseudo-scalar (F_P) form factor. Instead of PCAC, the axial Ward-Takahashi identity, $\partial_\alpha A_\alpha(x) = 2mP(x)$, leads to the generalized GT relation [2, 3]:

$$2M_N F_A(q^2) - q^2 F_P(q^2) = 2mG_P(q^2), \tag{2}$$

which is satisfied among the three nucleon form factors including the pseudoscalar (G_P) form factor defined in the pseudoscalar matrix element of the nucleon as

$$\langle N(p')|P(x)|N(p)\rangle = \bar{u}_N(p')\left[\gamma_5 G_P(q^2)\right]u_N(p)e^{iq\cdot x}. \tag{3}$$

In addition, the following pion-pole dominance (PPD) ansätz [4] for $F_P(q^2)$ and $G_P(q^2)$ at low q^2,

$$F_P^{\text{PPD}}(q^2) = \frac{2M_N F_A(q^2)}{q^2 + m_\pi^2} \quad \text{and} \quad 2mG_P^{\text{PPD}}(q^2) = 2M_N F_A(q^2)\frac{m_\pi^2}{q^2 + m_\pi^2}, \tag{4}$$

satisfies the generalized GT relation (2).

Although the axial-structure of the nucleon has been studied extensively in lattice QCD at the physical point, no results have been obtained that satisfy the generalized GT relation well or give better accuracy than the PPD model. Indeed, in our previous works [5, 6], both the F_P and G_P form factors are significantly underestimated in the low-q^2 region compared to the PPD model. This is simply due to strong πN excited-state contamination. In this work, we propose a simple method to remove the πN-state contamination from the F_P and G_P form factors, and then evaluate the induced pseudoscalar charge $g_P^* = m_\mu F_A(0.88m_\mu^2)$ and the pion-nucleon coupling $g_{\pi NN} = \lim_{q^2 \to \infty}(q^2 + m_\pi^2)\frac{F_P(q^2)}{2F_\pi}$ from existing data in a new analysis.

2. Standard method

The nucleon two-point (2pt) function from the source-time position (denoted t_{src}) to the sink-time position (denoted t_{sink}) is defined as

$$C_N(t_{\text{src}} - t_{\text{sink}}; \boldsymbol{p}) = \frac{1}{4}\text{Tr}\left\{\mathcal{P}_+\langle N(t_{\text{sink}}; \boldsymbol{p})\overline{N}(t_{\text{src}}; -\boldsymbol{p})\rangle\right\} \quad \text{with} \quad \mathcal{P}_+ = \frac{1+\gamma_4}{2}, \tag{5}$$

where the nucleon operator $N(t; \boldsymbol{q})$ carrying a three-dimensional momentum $\boldsymbol{p}$.

The nucleon form factors are extracted from the nucleon three-point (3pt) function consisting of the nucleon source and sink operators with a given local current (J) defined as

$$C_J^{5z}(t; \boldsymbol{p}', \boldsymbol{p}) = \frac{1}{4}\text{Tr}\left\{ \mathcal{P}^{5z}\langle N(t_{\text{sink}}; \boldsymbol{p}')J(t; \boldsymbol{q})\overline{N}(t_{\text{src}}; -\boldsymbol{p})\rangle \right\}, \tag{6}$$

where the projection operator $\mathcal{P}^{5z} = \mathcal{P}_{+}\gamma_5\gamma_3$ is chosen for $J = A_\alpha$ or P. We then calculate the following ratio constructed from an appropriate combination of the 2pt and 3pt functions [7, 8] with a fixed source-sink separation ($t_{\text{sep}} \equiv t_{\text{sink}} - t_{\text{src}}$):

$$\mathcal{R}_J^{5z}(t; \boldsymbol{p}', \boldsymbol{p}) = \frac{C_J^{5z}(t; \boldsymbol{p}', \boldsymbol{p})}{C_N(t_{\text{sink}} - t_{\text{src}}; \boldsymbol{p}')}\sqrt{\frac{C_N(t_{\text{sink}} - t; \boldsymbol{p})C_N(t - t_{\text{src}}; \boldsymbol{p}')C_N(t_{\text{sink}} - t_{\text{src}}; \boldsymbol{p}')}{C_N(t_{\text{sink}} - t; \boldsymbol{p}')C_N(t - t_{\text{src}}; \boldsymbol{p})C_N(t_{\text{sink}} - t_{\text{src}}; \boldsymbol{p})}}. \tag{7}$$

Since all t-dependence due to the contribution of the nucleon ground state can be eliminated in the ratio (7), the target quantity can be read off from an asymptotic plateau of the ratio $\mathcal{R}_J^{5z}(t; \boldsymbol{p}', \boldsymbol{p})$, being independent of the choice of t_{sep}, if the condition $t_{\text{sep}}/a \gg (t - t_{\text{src}})/a \gg 1$ is satisfied. In this study, we consider only the rest frame of the final state with $\boldsymbol{p}' = \boldsymbol{0}$, which leads to the condition of $\boldsymbol{q} = \boldsymbol{p} - \boldsymbol{p}' = \boldsymbol{p}$. Therefore, the squared four-momentum transfer is given by $q^2 = 2M_N(E_N(\boldsymbol{q}) - M_N)$ where M_N and $E_N(\boldsymbol{q})$ represent the nucleon mass and energy with the momentum $\boldsymbol{q}$. In this kinematics, we use a simpler notation like $\mathcal{R}_J^{5z}(t; \boldsymbol{q})$ and $C_J^{5z}(t; \boldsymbol{q})$.

The ratio $\mathcal{R}_J^{5z}(t; \boldsymbol{q})$ gives the following asymptotic values including the respective form factors in the asymptotic region [3]:

$$\mathcal{R}_{A_i}^{5z}(t; \boldsymbol{q}) = K^{-1}\left[(E_N(\boldsymbol{q}) + M_N)\widetilde{F}_A(q^2)\delta_{i3} - q_i q_3 \widetilde{F}_P(q^2) \right] + \cdots, \tag{8}$$

$$\mathcal{R}_{A_4}^{5z}(t; \boldsymbol{q}) = iq_3 K^{-1}\left[\widetilde{F}_A(q^2) - (E_N(\boldsymbol{q}) - M_N)\widetilde{F}_P(q^2) \right] + \cdots, \tag{9}$$

$$\mathcal{R}_P^{5z}(t; \boldsymbol{q}) = iq_3 K^{-1}\widetilde{G}_P\left(q^2\right) + \cdots, \tag{10}$$

with $K = \sqrt{2E_N(\boldsymbol{q})(E_N(\boldsymbol{q}) + M_N)}$. The ellipsis denotes excited-state contributions, which are supposed to be ignored in the case of $t_{\text{sep}}/a \gg (t - t_{\text{src}})/a \gg 1$. Three target quantities: $\widetilde{F}_A(q^2)$, $\widetilde{F}_P(q^2)$ and $\widetilde{G}_P(q^2)$ [1] can be read off from an asymptotic plateau of the ratio $\mathcal{R}_J^{5z}(t; \boldsymbol{q})$, being independent of the choice of t_{sep}. This approach is hereafter referred to as the standard method.

3. Simple subtraction method

In our previous works [5, 6, 9, 10], the 3pt functions involving the A_4 current are not taken into account for the calculation of the $F_A(q^2)$ and $F_P(q^2)$ form factors. This is simply because, to the best of our knowledge, the A_4 correlator was found to be statistically very noisy in Ref. [9], where the time-reversal averaging was performed using both forward and backward propagation in time for all 3pt functions. However, as pointed out for the first time in Ref. [11], the ratio correlator $\mathcal{R}_{A_4}^{5z}(t, \boldsymbol{q})$ does not show a plateau, but rather a peculiar behavior that depends linearly on the current insertion time t with a steep negative slope under their kinematic setup. When no time-reversal averaging is applied in our data, an almost linear t-dependence is indeed confirmed, giving the same slope, although the direction is reversed according to the respective kinematics.

---

[1]Hereafter, the form factors with and without tilde denote the bare and renormalized ones, then *e.g.* $F_A = Z_A\widetilde{F}_A$.
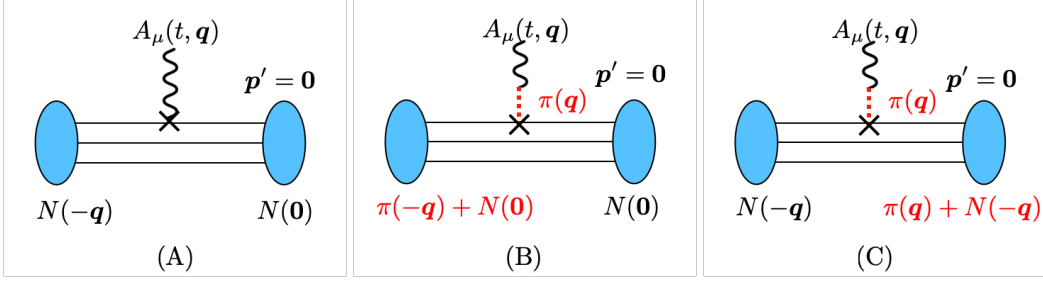
Figure 1: Schematic view of the ground-state contribution (A) and two types of the leading πN contributions (B) and (C) for the axial-vector matrix element.

As discussed in Ref. [12], such peculiar time dependence is understood as the leading contribution from the πN state in $\mathcal{R}_{A_4}^{5z}(t, \boldsymbol{q})$, arising in the tree diagram of the baryon ChPT. Importantly, the momentum $\boldsymbol{q}$ injected by the axial-vector current is entirely inherited by the pion state, since the pion in such πN state remains in the on-mass shell. The kinematics of the leading πN contribution is therefore restricted to two special cases as depicted in Fig. 1 (B) and (C) [13, 14].

In our previous works [5, 6, 9, 10], the F_P form factor obtained from $\widetilde{\mathcal{R}}_{A_i}^{5z}(t, \boldsymbol{q})$ was indeed significantly affected by the excited-state contamination, though no such effect was observed for the F_A form factor [2]. Therefore, we assume that the contributions from the leading πN state for $\mathcal{R}_{A_\alpha}^{5z}(t, \boldsymbol{q})$ can be described as follows

$$\widetilde{\mathcal{R}}_{A_i}^{5z}(t, \boldsymbol{q}) \equiv \mathcal{R}_{A_i}^{5z}(t, \boldsymbol{q}) - \delta_{i3}\mathcal{R}_{A_3}^{5z}(t, \boldsymbol{q}_0) = -q_3 q_i K^{-1}\left[\widetilde{F}_P(q^2) - \Delta_+(t, t_{\text{sep}}; \boldsymbol{q})\right], \tag{11}$$

$$\mathcal{R}_{A_4}^{5z}(t, \boldsymbol{q}) = iq_3 K^{-1}\left[\left(\widetilde{F}_A(q^2) - (E_N(\boldsymbol{q}) - M_N)\widetilde{F}_P(q^2)\right) + E_\pi(\boldsymbol{q})\Delta_-(t, t_{\text{sep}}; \boldsymbol{q})\right] \tag{12}$$

with $\boldsymbol{q}_0 = (q_1, q_2, 0)$ satisfying $|\boldsymbol{q}_0| = |\boldsymbol{q}|$. The functions $\Delta_\pm(t, t_{\text{sep}}; \boldsymbol{q})$ encode the leading πN contributions, which provide the residual t-dependence with a given t_{sep}.

For the case when the current operator carries the momentum $\boldsymbol{q}$, the πN contribution can be expressed by the following form with t-independent coefficients B and C

$$\Delta_\pm(t, t_{\text{sep}}; \boldsymbol{q}) = Be^{-\Delta E(\boldsymbol{q}, -\boldsymbol{q})t} \pm Ce^{-\Delta E(\boldsymbol{0}, \boldsymbol{q})(t_{\text{sep}}-t)}, \tag{13}$$

where the non-interaction estimates $\Delta E(\boldsymbol{q}, \boldsymbol{k}) = E_\pi(\boldsymbol{k}) + E_N(\boldsymbol{q} + \boldsymbol{k}) - E_N(\boldsymbol{q})$ may be used. Therefore, the time derivative of the πN contribution $\Delta_\pm(t, t_{\text{sep}}; \boldsymbol{q})$ may have the following property:

$$\partial_4 \Delta_\pm(t, t_{\text{sep}}; \boldsymbol{q}) = -E_\pi(\boldsymbol{q})\Delta_\mp(t, t_{\text{sep}}; \boldsymbol{q}) + (E_N(\boldsymbol{q}) - M_N)\Delta_\pm(t, t_{\text{sep}}; \boldsymbol{q}), \tag{14}$$

which offers us to separate the πN contribution $\Delta_\pm(t, t_{\text{sep}}; \boldsymbol{q})$ from the $\widetilde{F}_P$ form factor using the time-derivative of the ratio correlator $\partial_4 R_{A_\alpha}^{5z}(t; \boldsymbol{q})$. Hereafter the nucleon energy $E_N(\boldsymbol{q})$ and the pion energy $E_\pi(\boldsymbol{q})$ are simply abbreviated by shorthand notations E_N and E_π, respectively.

The new method for determining $\widetilde{F}_P(q^2)$, including the time derivative of the A_4 and A_i correlators, is given by

$$\widetilde{F}_P(q^2) = -K\frac{\widetilde{\mathcal{R}}_{A_i}^{5z}(t, \boldsymbol{q})}{q_i q_3} + \frac{K}{\Delta E_N^2 - E_\pi^2}\left[\Delta E_N\frac{\partial_4 \widetilde{\mathcal{R}}_{A_i}^{5z}(t, \boldsymbol{q})}{q_i q_3} + \frac{\partial_4 \mathcal{R}_{A_4}^{5z}(t, \boldsymbol{q})}{iq_3}\right] \tag{15}$$

---

[2]Recent studies solving the generalized eigenvalue problem including πN operators also show that the πN contributions are strong in $\widetilde{F}_P(q^2)$ and $\widetilde{G}_P(q^2)$, but not in $\widetilde{F}_A(q^2)$ [15, 16].

4

with $\Delta E_N \equiv E_N - M_N$ and $K = \sqrt{2E_N(E_N + M_N)}$. The first term corresponds to $\widetilde{F}_P^{\mathrm{std}}(q^2)$ in the standard method. The leading πN contributions represented in terms of $\Delta_+(t, t_{\mathrm{sep}}; \boldsymbol{q})$ and $\Delta_-(t, t_{\mathrm{sep}}; \boldsymbol{q})$ can be completely eliminated by adding the second term in Eq. (15). For the ground state contribution, namely $\widetilde{F}_P(q^2)$, Eq. (15) is just a harmless linear combination exploiting the redundancy in the determination of $\widetilde{F}_P(q^2)$ from both of $C_{A_4}^{5z}(t; \boldsymbol{q})$ and $C_{A_i}^{5z}(t; \boldsymbol{q})$. Therefore, if Eq. (15) successfully shows good plateau behavior, independent of the choice of t_{sep}, it guarantees that the ground state contribution can be read accurately without excited-state contamination.

Since the $\widetilde{G}_P(q^2)$ was also observed to be strongly contaminated from the excited state, similar to $\widetilde{F}_P(q^2)$, in our previous works [5, 6, 9, 10], we simply assume that

$$\mathcal{R}_P^{5z}(t, \boldsymbol{q}) = iq_3 K^{-1} \left[\widetilde{G}_P(q^2) - \Delta_P(t, t_{\mathrm{sep}}; \boldsymbol{q}) \right], \tag{16}$$

where $\Delta_P(t, t_{\mathrm{sep}}; \boldsymbol{q})$ encodes the leading πN state contributions that cause a residual t-dependence in $\mathcal{R}_P^{5z}(t; \boldsymbol{q})$. Unlike in the case of the axial-vector currents, only a single correlator cannot remove the πN contribution $\Delta_P(t, t_{\mathrm{sep}}; \boldsymbol{q})$. Instead, it was found that the axial Ward-Takahashi identity is well satisfied in terms of the 3pt functions of the nucleon in our previous study [6]:

$$Z_A[\partial_\alpha C_{A_\alpha}^{5z}(t; \boldsymbol{q})] = 2m_{\mathrm{PCAC}} C_P^{5z}(t; \boldsymbol{q}), \tag{17}$$

where m_{PCAC} corresponds to the bare quark mass which coincides with the value determined from the pion 2pt functions [6]. Recall that Eq. (17) is satisfied without isolating the ground-state contribution from the excited-state contributions [6]. Thus, Eq. (17) leads to the following PCAC relation for the leading πN contributions involved in $\tilde{\mathcal{R}}_{A_i}^{5z}(t; \boldsymbol{q})$ and $\mathcal{R}_P^{5z}(t; \boldsymbol{q})$:

$$\Delta_P(t, t_{\mathrm{sep}}; \boldsymbol{q}) = Z_A \frac{M_\pi^2}{2m_{\mathrm{PCAC}}} \Delta_+(t, t_{\mathrm{sep}}; \boldsymbol{q}), \tag{18}$$

which offers a simple subtraction method for determining the $\widetilde{G}_P(q^2)$ as below

$$\widetilde{G}_P(q^2) = K \frac{\mathcal{R}_P^{5z}(t, \boldsymbol{q})}{iq_3} + \frac{Z_A B_0 K}{\Delta E_N^2 - E_\pi^2} \left[\Delta E_N \frac{\partial_4 \tilde{\mathcal{R}}_{A_i}^{5z}(t, \boldsymbol{q})}{q_i q_3} + \frac{\partial_4 \mathcal{R}_{A_4}^{5z}(t, \boldsymbol{q})}{iq_3} \right] \tag{19}$$

with $B_0 = \frac{M_\pi^2}{2m_{\mathrm{PCAC}}}$. The first term corresponds to $\widetilde{G}_P^{\mathrm{std}}(q^2)$ in the standard method.

4. Numerical results

In this study, we reanalyze the data sets generated in Refs. [5, 6] for $\widetilde{F}_P(q^2)$ and $\widetilde{G}_P(q^2)$ using the new method described in Sec. 3. The two data sets are computed with the first and second

Table 1: Summary of simulation parameters in 2+1 flavor PACS10 ensembles with two different lattice spacings. See Refs. [6, 17, 18] for further details.

β	$L^3 \times T$	κ_{ud}	κ_s	c_{SW}	a^{-1} [GeV]	M_π [GeV]	Z_A^{SF}
1.82	$128^3 \times 128$	0.126117	0.124902	1.11	2.3	135	0.9650(68)
2.00	$160^3 \times 160$	0.125814	0.124925	1.02	3.1	138	0.9783(21)

PACS10 ensembles, which are two sets of gauge configurations generated in a large volume of about $(10 \text{ fm})^4$ by the PACS Collaboration with the six stout-smeared $O(a)$ improved Wilson-clover quark action and Iwasaki gauge action at $\beta = 1.82$ and 2.00 corresponding to the lattice spacings of 0.09 fm (coarse) and 0.06 fm (fine), respectively [5, 6]. A brief summary of the simulation parameters is given in Table 1. The simulated pion masses on both lattices are almost at the physical point.
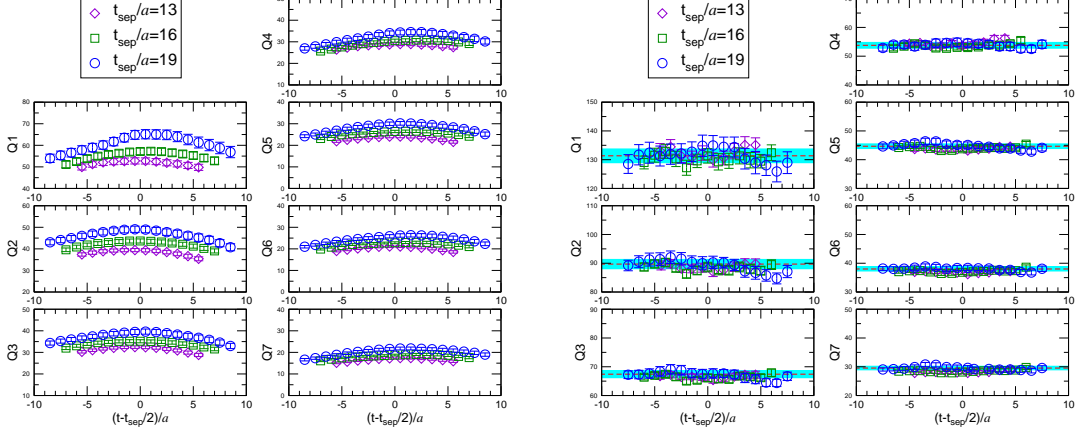
Figure 2: The values of $2M_N F_P^{\text{std}}$ (left) and $2M_N F_P$ (right) computed using the second PACS10 ensemble (160^4 lattice) with $t_{\text{sep}}/a = 13$ (diamonds), 16 (squares) and 19 (circles) for all momentum transfers as functions of the current insertion time slice t. In the right panel, the horizontal bands are calculated from the PPD model ($2M_N F_P^{\text{PPD}}(q^2)$).
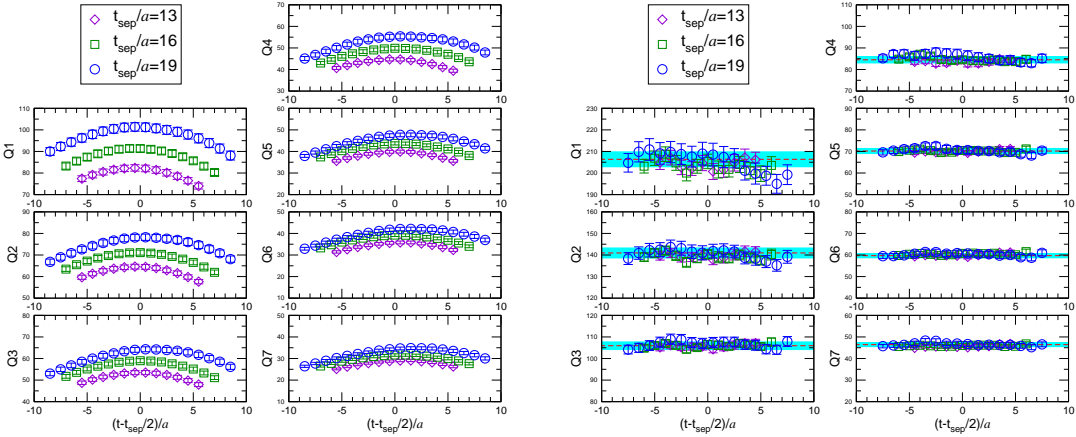
Figure 3: The values of $\widetilde{G}_P^{\text{std}}$ (left) and $\widetilde{G}_P$ (right) computed with $t_{\text{sep}}/a = 13$ (diamonds), 16 (squares) and 19 (circles) for all momentum transfers as functions of the current insertion time slice t. In the right panel, the horizontal bands are calculated from the PPD model ($\widetilde{G}_P^{\text{PPD}}(q^2)$).

The F_P form factor is extracted from Eq. (15) as a function of the current insertion time t. In Fig. 2, we compare the t-dependence and t_{sep}-dependence of $F_P(q^2)$ obtained by both the standard (left panel) and the simple subtraction (right panel) methods for the 160^4 lattice ensemble. The new method is really effective in obtaining an asymptotic plateau in all cases of $t_{\text{sep}}/a = \{13, 16, 19\}$ for

all q^2. Indeed, as shown in the right panel, the t-dependence is eliminated and the t_{sep}-dependence is not visible either. Furthermore, the plateau values are consistent with the PPD model.

As shown in Fig.3, similarly for the G_P form factor, the new method eliminates the slight convex shape associated with the excited-state contribution and yields a plateau behavior consistent with the PPD model without t_{sep} dependence as well. In Fig. 4, we plot the q^2 dependence of $2M_N F_P(q^2)$ (left panel) and $2m_{\text{PCAC}}\widetilde{G}_P(q^2)$ (right panel) for all data sets of 160^4 and 128^4 lattices together with experimental data points from muon capture [19] and pion-electro production [20].
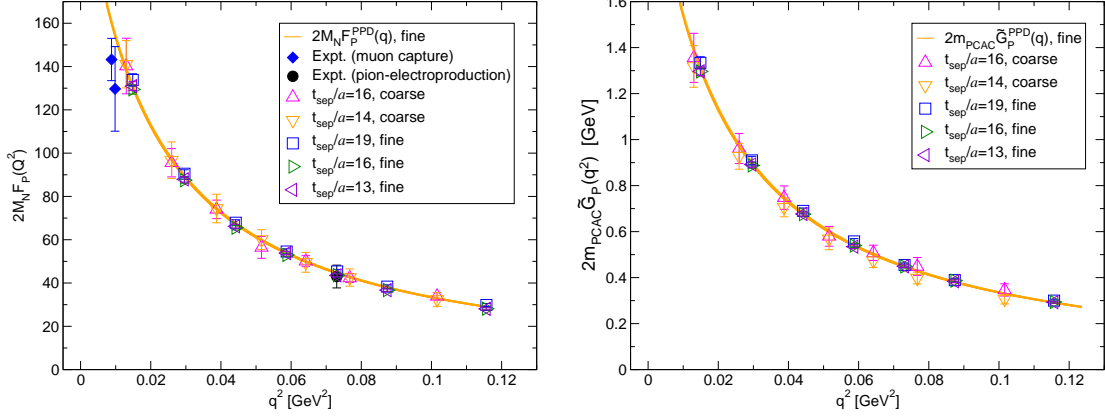
Figure 4: Results of $2M_N F_P(q^2)$ (left panel) and $2m_{\text{PCAC}}\widetilde{G}_P(q^2)$ (right panel) obtained by the new method as a function of q^2. In each panel, the solid curve is given by the PPD model defined in Eq. (4).

Next, g_P^* and $g_{\pi NN}$ are evaluated from the obtained F_P form factor according to the q^2 dependence analysis based on the z-expansion method applied to $(q^2 + m_\pi^2)F_P(q^2)$. As shown in Fig 5, no t_{sep} dependences are visible for either case and the discretization error on these quantities is less than 3-4 %, which is well controlled in our calculations as well as g_A. More importantly, the evaluation is possible with much smaller errors than the experimental values for g_P^* and comparable errors for $g_{\pi NN}$. Summary plots of our results together with the experimental values and other lattice QCD results for g_P^* and $g_{\pi NN}$ can be found in Ref. [21].

5. Summary

We have studied nucleon form factors in the axial-vector and pseudo-scalar channels in 2+1 flavor QCD using two sets of the PACS10 configurations at coarse and fine lattice spacings. Our simulations were carried out in very large spatial volumes, which allow us to access the low q^2 region, at the physical point essential for low-energy chiral behavior. The nucleon interpolating operator has been adopted with well-tuned smearing parameters that guarantee ground-state dominance in $F_A(q^2)$, although the two types of pseudo-scalar form factors, $F_P(q^2)$ and $G_P(q^2)$, still suffer from the excited-state contamination. In this study, we thus propose a simple subtraction method for removing the so-called leading πN-state contamination induced by the pion-pole structure appears in $F_P(q^2)$ and $G_P(q^2)$. The new method achieves the following points: 1) it can use the 3pt-functions of both spatial and temporal axial-vector currents to determine $F_P(q^2)$, 2) it is applicable for $G_P(q^2)$ with a help of the PCAC relation, 3) it eliminates both t-dependence and t_{sep}-dependence
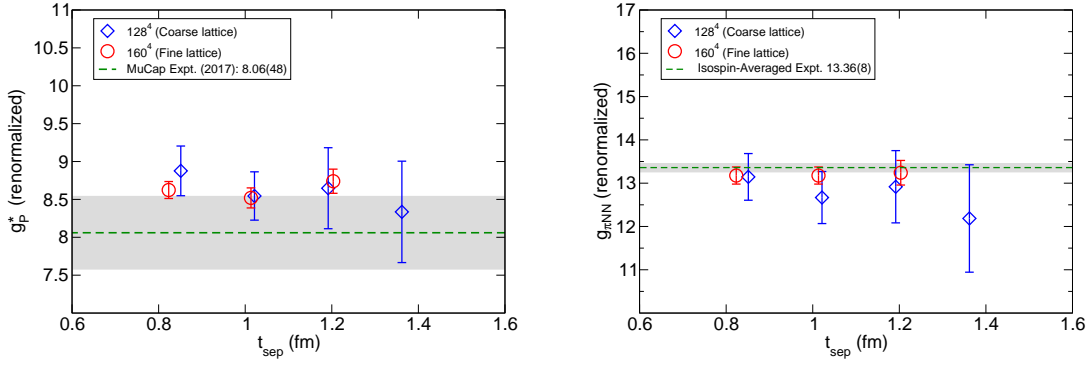
Figure 5: The source-sink separation (t_{sep}) dependence of the renormalized values of g_P^* (left) and $g_{\pi NN}$ (right). In each panel, the horizontal axis gives t_{sep} in physical units, while the horizontal dashed line with the gray band denotes the experimental value.

in both $F_P(q^2)$ and $G_P(q^2)$, 4) it makes results compatible with both the experiment and the PPD model, and 5) it provides more accurate results of two target quantities, g_P^* and $g_{\pi NN}$, comparing the multi-state analysis that was used in other groups [14, 22–24].

Acknowledgments

References

[1] M.L. Goldberger and S.B. Treiman, *Form-factors in Beta decay and muon capture*, *Phys. Rev.* **111** (1958) 354.

[2] W.I. Weisberger, *Unsubtracted Dispersion Relations and the Renormalization of the Weak Axial Vector Coupling Constants*, *Phys. Rev.* **143** (1966) 1302.

[3] S. Sasaki and T. Yamazaki, *Nucleon form factors from quenched lattice QCD with domain wall fermions*, *Phys. Rev. D* **78** (2008) 014510 [0709.3150].

[4] Y. Nambu, *Axial vector current conservation in weak interactions*, *Phys. Rev. Lett.* **4** (1960) 380.

[5] E. Shintani, K.-I. Ishikawa, Y. Kuramashi, S. Sasaki and T. Yamazaki, *Nucleon form factors and root-mean-square radii on a (10.8 fm)^4 lattice at the physical point*, *Phys. Rev. D* **99** (2019) 014510 [1811.07292].

[6] R. Tsuji, Y. Aoki, K.-I. Ishikawa, Y. Kuramashi, S. Sasaki, K. Sato et al., *Nucleon form factors in N_f=2+1 lattice QCD at the physical point: Finite lattice spacing effect on the root-mean-square radii*, *Phys. Rev. D* **109** (2024) 094505 [2311.10345].

[7] LHPC, SESAM collaboration, *Moments of nucleon generalized parton distributions in lattice QCD*, *Phys. Rev. D* **68** (2003) 034505 [hep-lat/0304018].

[8] QCDSF collaboration, *Nucleon electromagnetic form-factors on the lattice and in chiral effective field theory*, *Phys. Rev. D* **71** (2005) 034508 [hep-lat/0303019].

[9] PACS collaboration, *Nucleon form factors on a large volume lattice near the physical point in 2+1 flavor QCD*, *Phys. Rev. D* **98** (2018) 074510 [1807.03974].

[10] PACS collaboration, *Calculation of the derivative of nucleon form factors in Nf=2+1 lattice QCD at Mπ=138 MeV on a (5.5 fm)3 volume*, *Phys. Rev. D* **104** (2021) 074514 [2107.07085].

[11] G.S. Bali, S. Collins, M. Gruber, A. Schäfer, P. Wein and T. Wurm, *Solving the PCAC puzzle for nucleon axial and pseudoscalar form factors*, *Phys. Lett. B* **789** (2019) 666 [1810.05569].

[12] O. Bar, *Nπ-state contamination in lattice calculations of the nucleon axial form factors*, *Phys. Rev. D* **99** (2019) 054506 [1812.09191].

[13] H.B. Meyer, K. Ottnad and T. Schulz, *A new method for suppressing excited-state contaminations on the nucleon form factors*, *PoS* **LATTICE2018** (2018) 062 [1811.03360].

[14] RQCD collaboration, *Nucleon axial structure from lattice QCD*, *JHEP* **05** (2020) 126 [1911.13150].

[15] L. Barca, G. Bali and S. Collins, *Toward N to Nπ matrix elements from lattice QCD*, *Phys. Rev. D* **107** (2023) L051505 [`2211.12278`].

[16] C. Alexandrou, G. Koutsou, Y. Li, M. Petschlies and F. Pittler, *Investigation of pion-nucleon contributions to nucleon matrix elements*, *Phys. Rev. D* **110** (2024) 094514 [`2408.03893`].

[17] PACS collaboration, *Finite size effect on pseudoscalar meson sector in 2+1 flavor QCD at the physical point*, *Phys. Rev. D* **99** (2019) 014504 [`1807.06237`].

[18] PACS collaboration, *Finite size effect on vector meson and baryon sectors in 2+1 flavor QCD at the physical point*, *Phys. Rev. D* **100** (2019) 094502 [`1907.10846`].

[19] T. Gorringe and H.W. Fearing, *Induced Pseudoscalar Coupling of the Proton Weak Interaction*, *Rev. Mod. Phys.* **76** (2004) 31 [`nucl-th/0206039`].

[20] S. Choi et al., *Axial and pseudoscalar nucleon form-factors from low-energy pion electroproduction*, *Phys. Rev. Lett.* **71** (1993) 3927.

[21] R. Tsuji, Y. Aoki, K.-I. Ishikawa, Y. Kuramashi, S. Sasaki, K. Sato et al., *Studies of nucleon isovector structures with the PACS10 superfine lattice*, *PoS* **LATTICE2024** (2025) 318 [`2411.16784`].

[22] Nucleon Matrix Elements (NME) collaboration, *Precision nucleon charges and form factors using (2+1)-flavor lattice QCD*, *Phys. Rev. D* **105** (2022) 054505 [`2103.05599`].

[23] Precision Neutron Decay Matrix Elements (PNDME) collaboration, *Nucleon isovector axial form factors*, *Phys. Rev. D* **109** (2024) 014503 [`2305.11330`].

[24] Extended Twisted Mass collaboration, *Nucleon axial and pseudoscalar form factors using twisted-mass fermion ensembles at the physical point*, *Phys. Rev. D* **109** (2024) 034503 [`2309.05774`].